

Characteristic angular scales in cosmic microwave background radiation

F Ghasemi¹, A Bahraminasab², M Sadegh Movahed^{3,4},
Sohrab Rahvar^{3,5}, K R Sreenivasan⁶ and
M Reza Rahimi Tabar^{3,7}

¹ The Max Planck Institute for the Physics of Complex Systems, Nöthnitzer
Strasse 38, 01187 Dresden, Germany

² Department of Physics, Lancaster University, Lancaster LA1 4YB, UK

³ Department of Physics, Sharif University of Technology, PO Box 11365-9161,
Tehran, Iran

⁴ Institute for Studies in Theoretical Physics and Mathematics, PO Box
19395-5531, Tehran, Iran

⁵ Research Institute for Astronomy and Astrophysics of Maragha, PO Box
55134-441, Maragha, Iran

⁶ ICTP, Strada Costiera 11, I-34100 Trieste, Italy

⁷ CNRS UMR 6202, Observatoire de la Côte d'Azur, BP 4229, 06304 Nice
Cedex 4, France

E-mail: ghasemi@mpipks-dresden.mpg.de, a.bahraminasab@lancaster.ac.uk,
m.s.movahed@mehr.sharif.edu, rahvar@sharif.edu, krs@ictp.trieste.it and
rahimitabar@sharif.edu

Received 19 June 2006

Accepted 20 October 2006

Published 10 November 2006

Online at stacks.iop.org/JSTAT/2006/P11008

[doi:10.1088/1742-5468/2006/11/P11008](https://doi.org/10.1088/1742-5468/2006/11/P11008)

Abstract. We investigate the stochasticity in temperature fluctuations in the cosmic microwave background (CMB) radiation data from the *Wilkinson Microwave Anisotropy Probe*. We show that the angular fluctuation of the temperature is a Markov process with a *Markov angular scale*, $\Theta_{\text{Markov}} = 1.01^{+0.09}_{-0.07}$. We characterize the complexity of the CMB fluctuations by means of a Fokker–Planck or Langevin equation and measure the associated Kramers–Moyal coefficients for the fluctuating temperature field $T(\hat{n})$ and its increment, $\Delta T = T(\hat{n}_1) - T(\hat{n}_2)$. Through this method we show that temperature fluctuations in the CMB have fat tails compared to a Gaussian distribution.

Keywords: new applications of statistical mechanics

Contents

1. Introduction	2
2. Correlation angular scale from the joint PDF decomposition analysis	3
3. CMB data as a Markov process: least squares test	5
4. The (non-)Gaussianity test of CMB	9
5. Markov nature of the CMB and angular power spectrum	12
6. Conclusion	14
Acknowledgments	16
References	16

1. Introduction

The *Wilkinson Microwave Anisotropy Probe* (WMAP) mission is one of the main experiments on the cosmic microwave background (CMB), that determines the power spectrum of the temperature fluctuations in the CMB with high accuracy. It has been shown that the universe is geometrically flat, and that the dominant content of the universe is an exotic dark energy which causes the expansion of the universe to be accelerated [1]–[4]. The statistical properties of the CMB radiation are important tools for identifying the appropriate cosmological model and determining the parameters of the standard model [5]. The traditional way of studying the CMB data is through analysing their angular power spectrum and computing the two-point correlation function. In order to gain full statistical information from the temperature fluctuations on the last scattering surface, we should use the n -point joint probability density function (PDF) or the n -point correlation function.

At the same time, Gaussianity of the CMB anisotropy is an important question which is linked with the theoretical predictions made from the inflationary cosmology [6]–[8]. With current developments in experimental CMB physics, we are now in a position to analyse very large data sets that provide information about large patches of the sky, measured with very high resolution and sensitivity. This means that we can precisely test whether the CMB is Gaussian. Tantalizing evidence of non-Gaussianity has been emerging in the WMAP sky maps, using a variety of methods. The statistical properties of the primordial fluctuations generated by the inflationary cosmology are closely related to the anisotropy of the CMB radiation. Thus, measurement of the possible non-Gaussianity of the CMB data is a direct test of the inflation paradigm. If the CMB anisotropy is Gaussian, then the angular power spectrum, or the two-point correlation function, fully specifies its statistical properties.

In this paper we study the statistical properties of the CMB anisotropy through the n -point joint PDF of temperature fluctuations in the CMB data. We show that the fluctuations constitute a Markovian process with a Markov angular scale of $\Theta_{\text{Markov}} = 1.01^{+0.09}_{-0.07}$, or in the Legendre space, $l_{\text{Markov}} = 178.22^{+0.27}_{-0.21}$, at the 1σ confidence level. Using the Markov properties of the CMB data, a master equation for the angular evolution

of the probability distribution function—the Fokker–Planck (FP) equation—is obtained. To derive the relation between the standard power-spectral analysis and the Markov properties of the CMB data, we consider the joint probability distribution $P(T_2, \hat{n}_2; T_1, \hat{n}_1)$ that describes the probability of finding simultaneously T_1 in the direction $\hat{n}_1 = (\theta_1, \phi_1)$ and T_2 in the direction $\hat{n}_2 = (\theta_2, \phi_2)$. We then evaluate the corresponding Kramers–Moyal (KM) coefficients, and compute the first and second KM coefficients (i.e., the drift and diffusion coefficients in the FP equation). We show that the higher order coefficients in the KM expansion are very small and can be ignored. In addition, using the FP equation for the PDF, we show that temperature fluctuations on the last scattering surface are consistent with a Gaussian distribution. We also use the same analysis to investigate temperature fluctuations in the northern and southern hemispheres. The analysis detects some cold and hot spots in the southern and northern hemispheres, respectively.

The organization of this paper is as follows. In section 2 we determine the two-point joint PDF of temperature fluctuations and obtain the correlation angular scale. In section 3 we introduce the mathematical property of the PDF for the Markovian process and obtain the Markov angular scale for the WMAP data. We also develop the master equation in the form of a FP equation for the CMB data. In section 4 we investigate the (non-)Gaussian nature of the temperature fluctuations in the CMB. The relation between the Markov and the angular power spectrum for this set of data is obtained in section 5. The conclusions are presented in section 6.

2. Correlation angular scale from the joint PDF decomposition analysis

The WMAP instrument is composed of 10 differencing assemblies, spanning five frequencies from 23 to 94 GHz [9]. The two lowest frequency bands (K and Ka) are primarily galactic foreground monitors, while the three highest (Q, V, and W) are primarily cosmological bands. The full width at half-maximum for the detectors is a function of the frequency and ranges from 0.82° at 23 GHz to 0.21° at 94 GHz [10]. Here, we use the internal linear combination map which is a weighted linear combination of the five WMAP frequency maps. The weights are computed using the criterion that minimizes the galactic foreground contribution to the sky signal. The resultant map provides a low contamination image of the CMB anisotropy.

Let the temperature fluctuation in the CMB data in the direction of $\hat{n} = (\theta, \phi)$ be represented by $\mathcal{T}(\hat{n})$, and define $T(\hat{n}) \equiv (\mathcal{T}(\hat{n}) - \bar{T})/\sigma$, where \bar{T} and σ are the mean and variance of the temperature fluctuations, respectively. For a direction \hat{n}_0 with $T(\hat{n}_0) = T_0$, at any $\hat{n} \neq \hat{n}_0$, $T(\hat{n})$ is given by a PDF $P(T, \hat{n})$ (see figure 1). This means that $T(\hat{n})$ for $\hat{n} \neq \hat{n}_0$ is a stochastic (and possibly correlated) variable.

Complete information about the stochastic process is obtained from the knowledge about all the possible k -point or, more precisely, k -scale joint PDFs (JPDFs), $P(T_k, \hat{n}_k; T_{k-1}, \hat{n}_{k-1}; \dots; T_1, \hat{n}_1)$, describing the probability of finding simultaneously T_1 in the direction \hat{n}_1 , T_2 in the direction \hat{n}_2 , and so on up to T_k in the direction \hat{n}_k . Moreover, we can define the conditional probability distribution function. For a given $T(\hat{n}_0) = T_0$, the conditional probability for $T(\hat{n})$ at the successive positions $\hat{n}_1, \hat{n}_2, \dots, \hat{n}_k$ to be $T(\hat{n}_1), T(\hat{n}_2), \dots, T(\hat{n}_k)$ is described by

$$P_k^1(T_k, \hat{n}_k; \dots; T_1, \hat{n}_1 | T_0, \hat{n}_0) dT_k dT_{k-1} \dots dT_1 = \text{Prob}\{T(\hat{n}_i) \in [T_i, T_i + dT_i] \text{ for } i = 1, 2, \dots, k \text{ and } T(\hat{n}_0) = T_0\}. \quad (1)$$

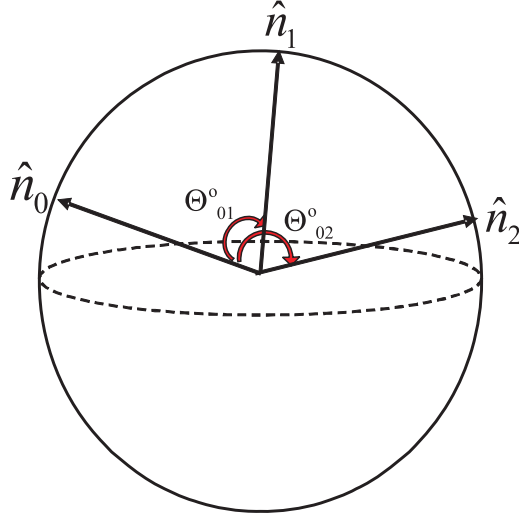


Figure 1. The arbitrary directions \hat{n}_0 , \hat{n}_1 and \hat{n}_2 in the sky to the last scattering surface.

In this notation, the superscript (for the P) represents the number of conditions (e.g., here, we have one condition), while the subscript denotes the number of stochastic variables in the joint PDF. The k -point JPDF of the temperature fluctuations is expressed by the product of the multiconditional PDFs as

$$\begin{aligned}
 & P(T_{k-1}, \hat{n}_{k-1}; T_{k-2}, \hat{n}_{k-2}; \dots; T_1, \hat{n}_1; T_0, \hat{n}_0) \\
 &= P_1^{k-1}(T_{k-1}, \hat{n}_{k-1} | T_{k-2}, \hat{n}_{k-2}; \dots; T_1, \hat{n}_1; T_0, \hat{n}_0) \\
 &\quad \times P_1^{k-2}(T_{k-2}, \hat{n}_{k-2} | T_{k-3}, \hat{n}_{k-3}; \dots; T_1, \hat{n}_1; T_0, \hat{n}_0) \\
 &\quad \times \dots \times P_1^1(T_1, \hat{n}_1 | T_0, \hat{n}_0) P(T_0, \hat{n}_0)
 \end{aligned} \tag{2}$$

where $P_1^1(T_1, \hat{n}_1 | T_0, \hat{n}_0)$ denotes a conditional probability of finding temperature fluctuation T_1 in the direction \hat{n}_1 , under the condition that the temperature T_0 in the direction \hat{n}_0 has been found. This conditional probability can be expressed by a two-point JPDF, as $P_1^1(T_1, \hat{n}_1 | T_0, \hat{n}_0) = P(T_1, \hat{n}_1; T_0, \hat{n}_0) / P(T_0, \hat{n}_0)$; this result is important because, if the conditional PDF for the T_1 is independent of T_0 , then $P_1^1(T_1, \hat{n}_1 | T_0, \hat{n}_0) = P(T_1, \hat{n}_1)$ and, in this case, $P_1^1(T_1, \hat{n}_1; T_0, \hat{n}_0) = P(T_1, \hat{n}_1)P(T_0, \hat{n}_0)$.

To derive the first characteristic angular scales in the CMB, we define the *correlation angular scale*, where the JPDF can be decomposed as the product of two independent PDFs [11] as

$$P(T_2, \hat{n}_2; T_1, \hat{n}_1) |_{\Theta_C} = P(T_1, \hat{n}_1) P(T_2, \hat{n}_2). \tag{3}$$

Here, Θ is the angular separation between the two directions \hat{n}_1 and \hat{n}_2 , and we assumed statistical isotropy of the temperature fluctuations in the CMB in which the correlation function depends only on the angle between the two directions of \hat{n}_1 and \hat{n}_2 [12]. In figure 2 we plot $\Delta P(T_2, T_1) = |P(T_2, \hat{n}_2; T_1, \hat{n}_1) - P(T_1, \hat{n}_1)P(T_2, \hat{n}_2)|$ in terms of Θ , using the least squares method:

$$\chi^2 = \int \frac{[P(T_2, \hat{n}_2; T_1, \hat{n}_1) - P(T_1, \hat{n}_1)P(T_2, \hat{n}_2)]^2}{\sigma_{\text{PDF}}^2 + \sigma_{2\text{-joint}}^2} dT_1 dT_2,$$

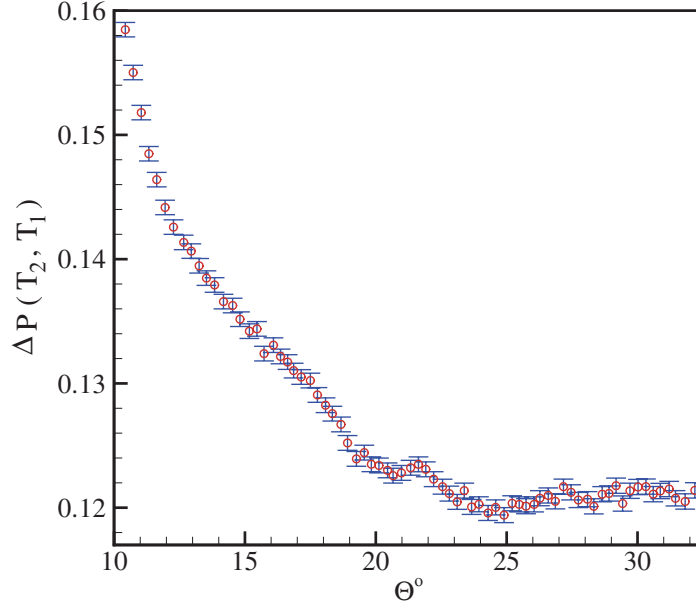


Figure 2. Θ is the angular separation between two directions \hat{n}_1 and \hat{n}_2 . For $\Theta_C = 24.86^\circ \pm 0.03$ we obtain the minimum value for $\Delta P(T_2, T_1) = |P(T_2, \hat{n}_2; T_1, \hat{n}_1) - P(T_1, \hat{n}_1)P(T_2, \hat{n}_2)|$ versus Θ .

where the minimum value of χ^2 corresponds to the angular scale at which the correlation disappears. Here, σ_{PDF}^2 and $\sigma_{2\text{-joint}}^2$ are the variances of $P(T_1, \hat{n}_1)P(T_2, \hat{n}_2)$ and $P(T_2, \hat{n}_2; T_1, \hat{n}_1)$, respectively. Our analysis indicates that the minimum value of $\Delta P(T_2, T_1)$ happens at $\Theta_C = 24.86^\circ \pm 0.03$ with $\chi_\nu^2 = 1.01$ ($\chi_\nu^2 = \chi^2/\mathcal{N}$, with \mathcal{N} being the number of degrees of freedom).

3. CMB data as a Markov process: least squares test

Now, let us check whether the CMB data follow a Markov chain and, if they do, measure the second characteristic angular scale in the CMB, i.e., the Markov angular scale Θ_{Markov} —the scale over which the CMB data are Markov correlated. In other words, the Markov angular scale Θ_{Markov} is the minimum angular separation over which the data can be represented by a Markov process [13]–[15]. The exact mathematical definition of the Markov process is given [16] by

$$P(T_k, \hat{n}_k | T_{k-1}, \hat{n}_{k-1}; \dots; T_1, \hat{n}_1; T_0, \hat{n}_0) = P(T_k, \hat{n}_k | T_{k-1}, \hat{n}_{k-1}). \quad (4)$$

Intuitively, the physical interpretation of a Markov process is that it ‘forgets its past’, or, in other words, only the most nearby conditioning, say (T_k, \hat{n}_k) , is relevant to the probability of finding a temperature T_k at \hat{n}_k . In the Markov process the ability to predict the value of $T(\hat{n})$ will not be enhanced by knowing its values in the steps prior to the most recent one. Therefore, an important simplification that can be made for a Markov process is that a conditional multivariate JPDF (equation (2)) can be written in terms of the products of simple two-parameter conditional PDFs [16] as

$$P(T_k, \hat{n}_k; T_{k-1}, \hat{n}_{k-1}; \dots; T_1, \hat{n}_1 | T_0, \hat{n}_0) = \prod_{i=1}^k P(T_i, \hat{n}_i | T_{i-1}, \hat{n}_{i-1}). \quad (5)$$

In what follows, we use the least squares method to determine the Markov angular scale of the CMB temperature fluctuations. Testing equation (4) for large values of k is beyond of our computational capability; however, for $k = 3$, where we have three vectors giving the 2D celestial sphere, the Markov condition is as follows:

$$P(T_3, \hat{n}_3 | T_2, \hat{n}_2; T_1, \hat{n}_1) = P(T_3, \hat{n}_3 | T_2, \hat{n}_2), \quad (6)$$

where $\Theta_{ij} = \arccos(\hat{n}_i \cdot \hat{n}_j)$ is the separation angle of \hat{n}_i and \hat{n}_j , and $\Theta_{31} > \Theta_{32}, \Theta_{21}$ (see figure 1). For simplicity, we let $\Theta_{21} = \Theta_{32}$. A process is Markovian if equation (6) is satisfied for a certain angular separation which, in our notation, is Θ_{32} . We refer to it as the Markov angular scale (Θ_{Markov}).

In order to determine the Markov angular scale, we compare the three-point PDF with that obtained on the basis of the Markov process. The three-point PDF, in terms of conditional probability functions, is given by

$$P(T_3, \hat{n}_3; T_2, \hat{n}_2; T_1, \hat{n}_1) = P(T_3, \hat{n}_3 | T_2, \hat{n}_2; T_1, \hat{n}_1) P(T_2, \hat{n}_2; T_1, \hat{n}_1). \quad (7)$$

Using the properties of the Markov process and substituting in equation (6) we obtain

$$P_{\text{Mar}}(T_3, \hat{n}_3; T_2, \hat{n}_2; T_1, \hat{n}_1) = P(T_3, \hat{n}_3 | T_2, \hat{n}_2) P(T_2, \hat{n}_2; T_1, \hat{n}_1). \quad (8)$$

In order to check the condition for the data being a Markov process, we must compute the three-point JPDF through equation (7) and compare the result with equation (8). The first step in this direction is to determine the quality of the fit through the least squares fitting quantity χ^2 defined by

$$\chi^2 = \int dT_3 dT_2 dT_1 [P(T_3, \hat{n}_3; T_2, \hat{n}_2; T_1, \hat{n}_1) - P_{\text{Mar}}(T_3, \hat{n}_3; T_2, \hat{n}_2; T_1, \hat{n}_1)]^2 / [\sigma_{3\text{-joint}}^2 + \sigma_{\text{Mar}}^2] \quad (9)$$

where $\sigma_{3\text{-joint}}^2$ and σ_{Mar}^2 are the variances of $P(T_3, \hat{n}_3; T_2, \hat{n}_2; T_1, \hat{n}_1)$ and $P_{\text{Mar}}(T_3, \hat{n}_3; T_2, \hat{n}_2; T_1, \hat{n}_1)$, respectively. To compute the Markov angular scale, we use the likelihood statistical analysis [17]. In the absence of a prior constraint, the probability of the set of three-point JPDFs is given by a product of Gaussian functions:

$$p(\arccos(\hat{n}_3, \hat{n}_2)) = \prod_{T_3, T_2, T_1} \frac{1}{\sqrt{2\pi(\sigma_{3\text{-joint}}^2 + \sigma_{\text{Mar}}^2)}} \times \exp \left[-\frac{[P(T_3, \hat{n}_3; T_2, \hat{n}_2; T_1, \hat{n}_1) - P_{\text{Mar}}(T_3, \hat{n}_3; T_2, \hat{n}_2; T_1, \hat{n}_1)]^2}{2(\sigma_{3\text{-joint}}^2 + \sigma_{\text{Mar}}^2)} \right]. \quad (10)$$

This probability distribution must be normalized. Evidently, when, for a set of values of the parameters, the χ^2 is minimum, the probability is maximum. Figure 3 shows the normalized χ^2_{ν} as a function of the angular length scale $\Theta = \Theta_{32} \equiv \arccos(\hat{n}_3 \cdot \hat{n}_2)$. The minimum value of χ^2_{ν} is 1.38, corresponding to $\Theta_{\text{Markov}} = 1.01_{-0.07}^{+0.09}$ with a 1σ confidence level. Figure 4 shows the likelihood function of the Markov angular scale of the CMB.

The Markov nature of the CMB enables us to derive a master equation—a FP equation—for the evolution of the PDF $P(T, \hat{n})$, in terms of, for example, the direction \hat{n} . One writes equation (8) as an integral equation, which is well known as the Chapman–Kolmogorov (CK) equation:

$$P(T_3, \hat{n}_3 | T_1, \hat{n}_1) = \int dT_2 P(T_3, \hat{n}_3 | T_2, \hat{n}_2) P(T_2, \hat{n}_2 | T_1, \hat{n}_1). \quad (11)$$

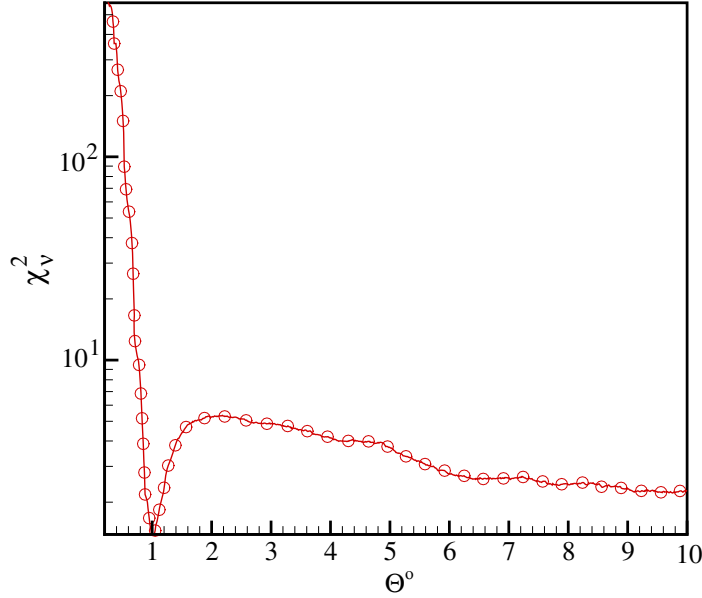


Figure 3. χ_ν^2 in terms of the angular scale Θ . The minimum value of $\chi_\nu^2 = 1.388$ corresponds to $\Theta_{\text{Markov}} = 1.01_{-0.07}^{+0.09}$, with a 1σ confidence level.

We checked the validity of the CK equation for describing the angular separation of \hat{n}_1 and \hat{n}_2 being equal to the Markov angular scale. This is shown in figure 5. In the upper panel we show the identification of the left (filled symbol) and right (open symbol) sides of equation (11) for three levels, 0.008 (red symbol), 0.005 (blue symbol), 0.002 (green symbol). The conditional PDFs $P(T_3|T_1)$ for $T_1 = \pm\sigma$ are shown in the lower panel. All the scales are measured in units of the standard deviation of the temperature fluctuations. The CK equation, formulated in differential form, yields the following Kramers–Moyal (KM) expansion [16]:

$$\frac{\partial}{\partial\phi}P(T, \phi) = \sum_{n=1}^{\infty} \left(-\frac{\partial}{\partial T}\right)^n [D^{(n)}(T, \phi)P(T, \phi)], \quad (12)$$

where $D^{(n)}(T, \phi)$ are called the KM coefficients. These coefficients can be estimated directly from the moments ($M^{(n)}$) and the conditional probability distributions as

$$\begin{aligned} D^{(n)}(T, \phi) &= \frac{1}{n!} \lim_{\Delta\phi \rightarrow 0} M^{(n)}, \\ M^{(n)} &= \frac{1}{\Delta\phi} \int dT' (T' - T)^n P(T', \phi + \Delta\phi|T, \phi). \end{aligned} \quad (13)$$

According to Pawula’s theorem [16], for a process with $D^{(4)} \sim 0$, all the $D^{(n)}$ with $n \geq 3$ vanish, and the KM expansion reduces to the FP equation, known also as the Kolmogorov equation [16]:

$$\frac{\partial}{\partial\phi}P(T, \phi) = \left[-\frac{\partial}{\partial T}D^{(1)}(T, \phi) + \frac{\partial^2}{\partial T^2}D^{(2)}(T, \phi)\right] P(T, \phi). \quad (14)$$

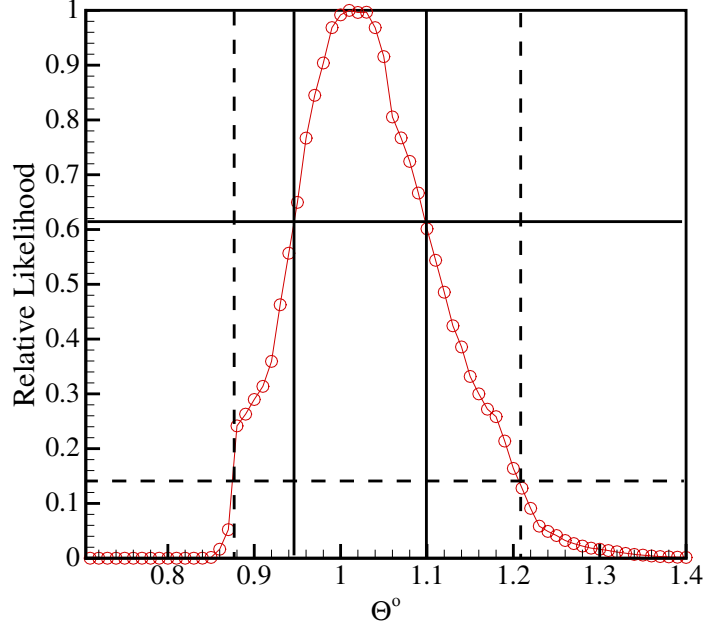


Figure 4. Relative likelihood function for the Markov angular scale of the CMB fluctuations, as a function of Θ . The intersections of the curve with the horizontal solid and dashed lines give the bounds with 1σ and 2σ confidence levels, respectively. The minimum value of $\chi^2_\nu = 1.38$ corresponds to $\Theta_{\text{Markov}} = 1.01^{+0.09}_{-0.07}$, with 1σ and $\Theta_{\text{Markov}} = 1.01^{+0.19}_{-0.13}$, with a 2σ confidence level.

Here $D^{(1)}(T, \phi)$ is the ‘drift’ term, describing the deterministic part of the process, while $D^{(2)}(T, \phi)$ is the ‘diffusion’ term. Using the Ito interpretation, the FP equation is equivalent to the following Langevin equation [16]:

$$\frac{d}{d\phi}T(\phi) = D^{(1)}(T) + \sqrt{D^{(2)}(T)}f(\phi). \quad (15)$$

Here, $f(\phi)$ is a δ -correlated Gaussian random force with zero mean (i.e., $\langle f(\phi)f(\phi') \rangle = 3D\delta(\phi - \phi')$). For the WMAP data, the drift and diffusion coefficients $D^{(1)}$ and $D^{(2)}$ are shown in figure 6. It turns out that the drift coefficient $D^{(1)}$ is a linear function in T , whereas the diffusion coefficient $D^{(2)}$ is a quadratic function. For large values of T , our estimates become poor and, thus, the uncertainty increases. From the analysis of the data set, we obtain the following approximate relations:

$$\begin{aligned} D^{(1)}(T) &= -0.330T, \\ D^{(2)}(T) &= 0.060T^2 + 0.002T + 0.270, \end{aligned} \quad (16)$$

where we used the isotropy assumption which implies that $D^{(n)}(T, \phi) = D^{(n)}(T)$. The temperature field is measured in units of its standard deviation. The fourth-order coefficient $D^{(4)}$ is, in our analysis, $D^{(4)} \simeq 10^{-2}D^{(2)}$, so we can ignore the coefficients $D^{(n)}$ for $n \geq 3$. Furthermore, using equation (15), it becomes clear that we are able to separate the deterministic and the noisy components of the CMB fluctuations in terms of the coefficients $D^{(1)}$ and $D^{(2)}$.

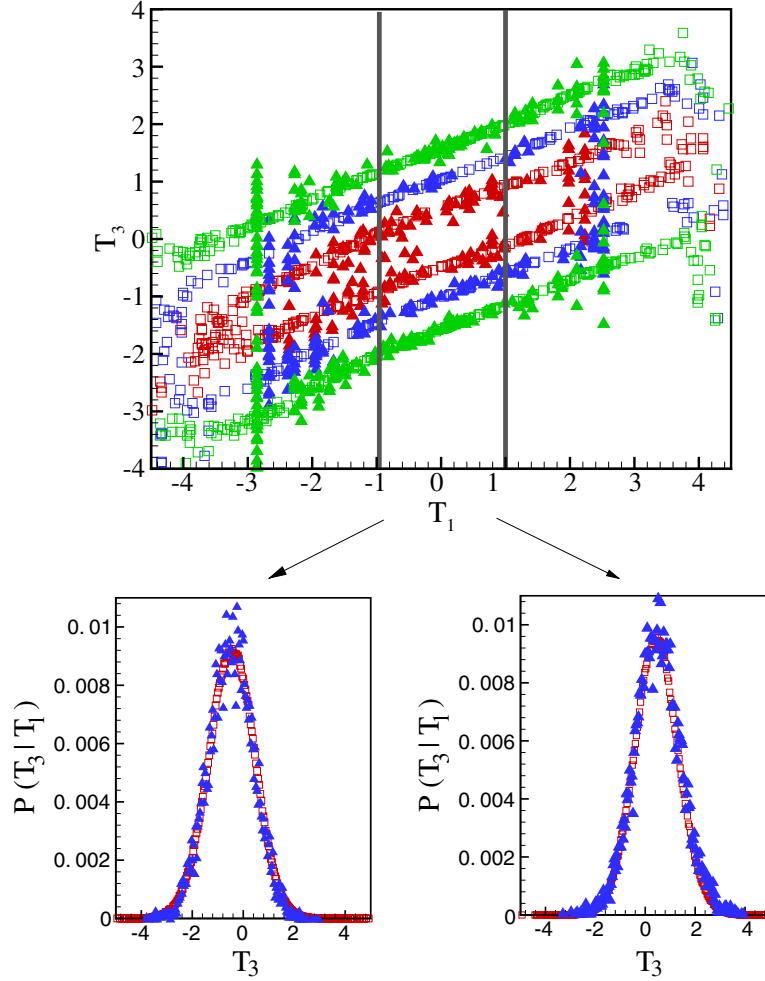


Figure 5. Verification of the validity of the Chapman–Kolmogorov equation (equation (11)) for the angular separation of \hat{n}_1 and \hat{n}_2 being equal to the Markov angular scale. In the upper panel we show the identification of left (filled symbol) and right (open symbol) sides of equation (11) for three levels, 0.008 (red symbol), 0.005 (blue symbol), 0.002 (green symbol). The conditional PDFs $P(T_3|T_1)$ for $T_1 = \pm\sigma$ are shown in the lower panel. All the scales are measured in units of the standard deviation of the temperature fluctuations.

4. The (non-)Gaussianity test of CMB

Cosmological models of the structure formation are based on the standard inflationary paradigm, which implies Gaussian fluctuation of the density field [6]–[8], [18]. The Gaussianity in the density perturbation directly translates into the Gaussianity of the CMB temperature fluctuations. However, along with the standard inflationary models, there exist theories that predict non-Gaussianity of the primordial fluctuations. Inflation with two or more scalar fields can provide significant deviations from the Gaussianity [19]–[22]. Another possibility is the manipulation of the CMB data after the recombination, due to subsequent weak gravitational lensing [23, 24] and various foregrounds, such as

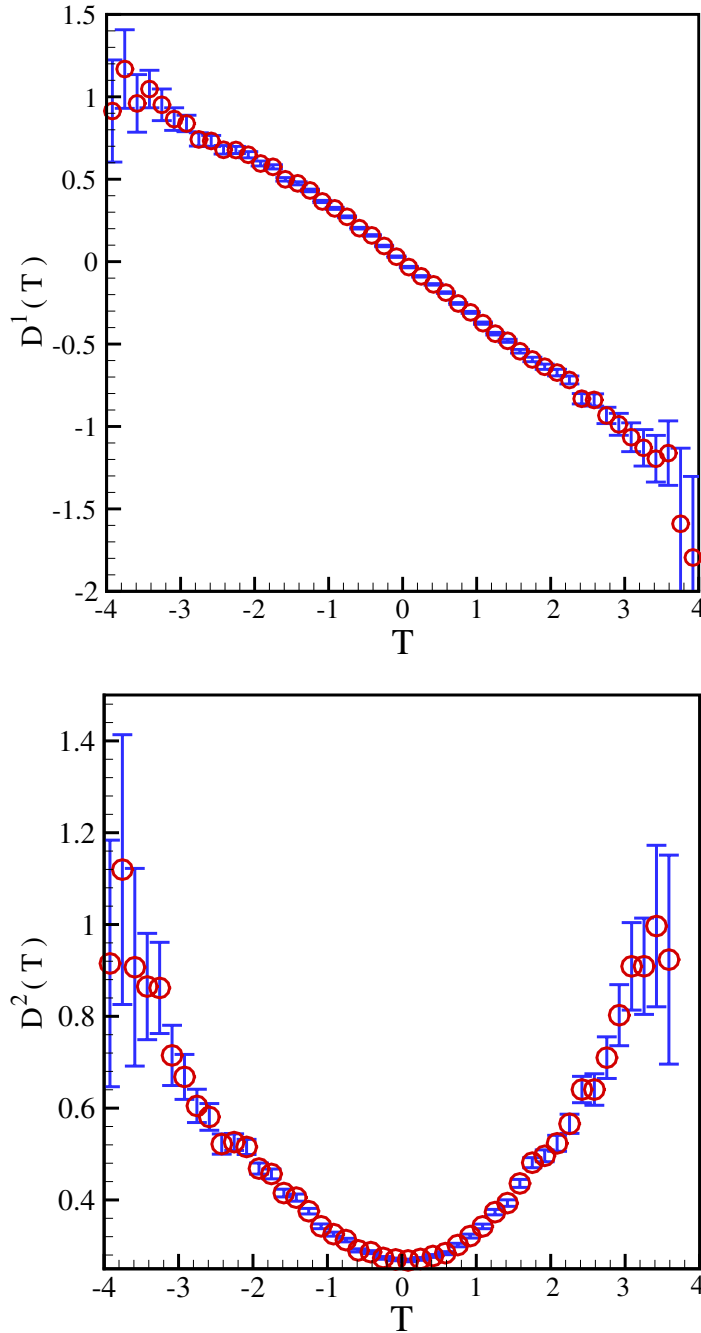


Figure 6. The drift and diffusion coefficients, $D^{(1)}(T)$ and $D^{(2)}(T)$ in equation (13), following, respectively, linear and quadratic behaviours.

dust emission, synchrotron radiation, and unresolved point sources [25]. One should also take into account the additional instrumental noise in the observational data [26].

There are standard methods of searching for non-Gaussian signature in the CMB data, such as using peak distributions [18, 27], the genus curve [28, 29], peak correlations [30] and global Minkowski functional methods [31]. More recent methods, such as a technique for

Table 1. The values of moments $\langle T^n \rangle$ for the whole sphere, the northern and the southern hemispheres of the CMB map data.

	$\langle T^2 \rangle$	$\langle T^3 \rangle$
Whole sphere	$(5.588 \pm 0.005) \times 10^{-3}$	$(-2.033 \pm 0.108) \times 10^{-5}$
Northern hemisphere	$(4.914 \pm 0.006) \times 10^{-3}$	$(1.283 \pm 0.125) \times 10^{-5}$
Southern hemisphere	$(6.264 \pm 0.007) \times 10^{-3}$	$(-5.408 \pm 0.175) \times 10^{-5}$
	$\langle T^4 \rangle$	$\langle T^5 \rangle$
Whole sphere	$(1.009 \pm 0.003) \times 10^{-4}$	$(-1.298 \pm 0.132) \times 10^{-6}$
Northern hemisphere	$(7.867 \pm 0.0305) \times 10^{-5}$	$(7.632 \pm 1.028) \times 10^{-7}$
Southern hemisphere	$(1.233 \pm 0.005) \times 10^{-4}$	$(-3.392 \pm 0.244) \times 10^{-6}$

studying hydrodynamic turbulence and detecting non-Gaussianity, and fractal analysis, can also be used for the CMB data [32, 33]. Moreover, the Gaussianity of the CMB at different angular scales has been tested [34]–[57]. Most of the previous works were based on the consistency between the CMB data and simulated Gaussian realizations. So far, they have found no significant evidence for cosmological non-Gaussianity.

We note that for a Gaussian distribution, all the even moments are related to the second one through $\langle T^{2n} \rangle = (2n!/2^n n!) \langle T^2 \rangle^n$ (e.g., for $n = 2$, $\langle T^4 \rangle = 3 \langle T^2 \rangle^2$), while the odd moments are zero. We checked directly the relation between the moments for the CMB data. The results are summarized in table 1. The ratios $\langle T^4 \rangle / (3 \langle T^2 \rangle^2)$ are 1.077 ± 0.004 , 1.085 ± 0.005 and 1.048 ± 0.005 , for the entire data set, and the northern and southern hemispheres, respectively. The odd moments $\langle T^3 \rangle$ and $\langle T^5 \rangle$ are not zero for different parts of the CMB data (see table 1). The odd moments of the temperature fluctuations can also be used as the indicators for the hot and cold spots. The southern part has a negative third moment, indicating greater prevalence of the cold spots, whereas the northern hemisphere has a positive third moment, indicating domination of the hot spots. The ratios of the higher moments, such as $\langle T^6 \rangle / (15 \langle T^2 \rangle^3)$, are 1.398 ± 0.026 , 1.396 ± 0.022 and 1.313 ± 0.035 (for a Gaussian distribution this ratio is unity) for the entire data set, and the northern and southern hemispheres, respectively.

The ratio of the higher moments, such as $\langle T^6 \rangle / (15 \langle T^2 \rangle^3)$, for the entire sky, and the northern and southern hemispheres are larger than those for a Gaussian distribution, implying that the probability distribution function for the temperature fluctuations in the CMB has fat tails compared to a Gaussian distribution.

Let us examine the predictions for the moments of the temperature fluctuations via the FP equation, and compare their values with the direct evaluation of results presented in table 1. Using the stochastic properties of the temperature field, one can check the deviation of the fluctuations from the Gaussian distribution in the northern and southern hemispheres, as well as in the entire data. As pointed out in section 3, the PDF of the temperature fluctuations satisfies the KM expansion. Using equation (12) we calculate the n th moment of the temperature fluctuations by multiplying both sides of equation (12) by T^n and integrating over the temperature:

$$\frac{d}{d\phi} \langle T^n \rangle = \sum_{m=1}^{\infty} \frac{n!}{(n-m)!} \langle D^{(m)}(T) T^{n-m} \rangle. \quad (17)$$

Table 2. The values of Kramers–Moyal coefficients for the northern and the southern hemispheres of the CMB map data.

	$D^{(1)}(T)$	$D^{(2)}(T)$	$D^{(3)}(T)$	$D^{(4)}(T)$
Northern hemisphere	$-0.370T$	$0.290 - 0.003T + 0.075T^2$	$-0.001 - 0.110T + 0.003T^2 - 0.010T^3$	$0.040 - 0.007T + 0.0182T^2 - 0.0005T^3 + 0.001T^4$
Southern hemisphere	$-0.290T$	$0.250 + 0.007T + 0.047T^2$	$0.004 - 0.078T - 0.005T^2 - 0.003T^3$	$0.031 - 0.003T + 0.020T^2 + 0.001T^3 - 0.001T^4$

We set $n = 4$ in the above equation and find the equation for the fourth moment to be

$$\frac{d}{d\phi}\langle T^4 \rangle = 4\langle D^{(1)}(T)T^3 \rangle + 12\langle D^{(2)}(T)T^2 \rangle + 24\langle D^{(3)}(T)T \rangle + 24\langle D^{(4)}(T) \rangle. \quad (18)$$

The KM coefficients for the northern and the southern hemispheres are given in table 2. For the isotropic case, all the moments of temperature fluctuations are independent of ϕ , and the left-hand side of equation (18) vanishes. Using the results presented in table 2, for the northern and the southern hemispheres, equation (18) reduces to

$$\begin{aligned} \langle T^4 \rangle_{\text{north}} &= (2.71 \pm 0.06)\langle T^2 \rangle^2 + (0.028 \pm 0.010)\langle T^3 \rangle\sqrt{\langle T^2 \rangle}, \\ \langle T^4 \rangle_{\text{south}} &= (3.27 \pm 0.09)\langle T^2 \rangle^2 - (0.017 \pm 0.020)\langle T^3 \rangle\sqrt{\langle T^2 \rangle}, \end{aligned} \quad (19)$$

where for the northern and southern hemispheres, $\langle T^3 \rangle = (1.283 \pm 0.125) \times 10^{-5}$, $\sqrt{\langle T^2 \rangle} = (7.010 \pm 0.004) \times 10^{-2}$ and $\langle T^3 \rangle = (-5.408 \pm 0.175) \times 10^{-5}$, $\sqrt{\langle T^2 \rangle} = (7.914 \pm 0.004) \times 10^{-2}$, respectively. We repeated the same procedure for the entire data set and obtained the following relation between the moments:

$$\langle T^4 \rangle = (3.07 \pm 0.07)\langle T^2 \rangle^2 + (0.034 \pm 0.020)\langle T^3 \rangle\sqrt{\langle T^2 \rangle}, \quad (20)$$

where $\langle T^3 \rangle = (-2.032 \pm 0.108) \times 10^{-5}$ and $\sqrt{\langle T^2 \rangle} = (7.475 \pm 0.003) \times 10^{-2}$. The drift and diffusion coefficients of the northern and the southern hemispheres are shown in figure 7.

As mentioned earlier, for a Gaussian distribution, all the even moments are related to the second one, while the odd moments are zero. Equations (19) and (20) show that we have deviations from Gaussianity, resulting from the coefficient of $\langle T^2 \rangle^2$. Note that the results presented by equation (20) are compatible with direct calculations of moments for different parts of the CMB data.

5. Markov nature of the CMB and angular power spectrum

Using statistical isotropy, the two-point temperature correlation function is expanded in terms of the Legendre functions as

$$\langle T(\hat{n}_1)T(\hat{n}_2) \rangle = \sum_l \frac{2l+1}{4\pi} C_l P_l(\cos(\Theta)), \quad (21)$$

where C_l is the angular power spectrum, P_l is the Legendre polynomial of order l and $\Theta = \arccos(\hat{n}_1 \cdot \hat{n}_2)$. To find the relation between the Markovian properties of the CMB data and the C_l , we start with the temperature increment moments, $S_2 = \langle [T(\hat{n}_1) - T(\hat{n}_2)]^2 \rangle$.

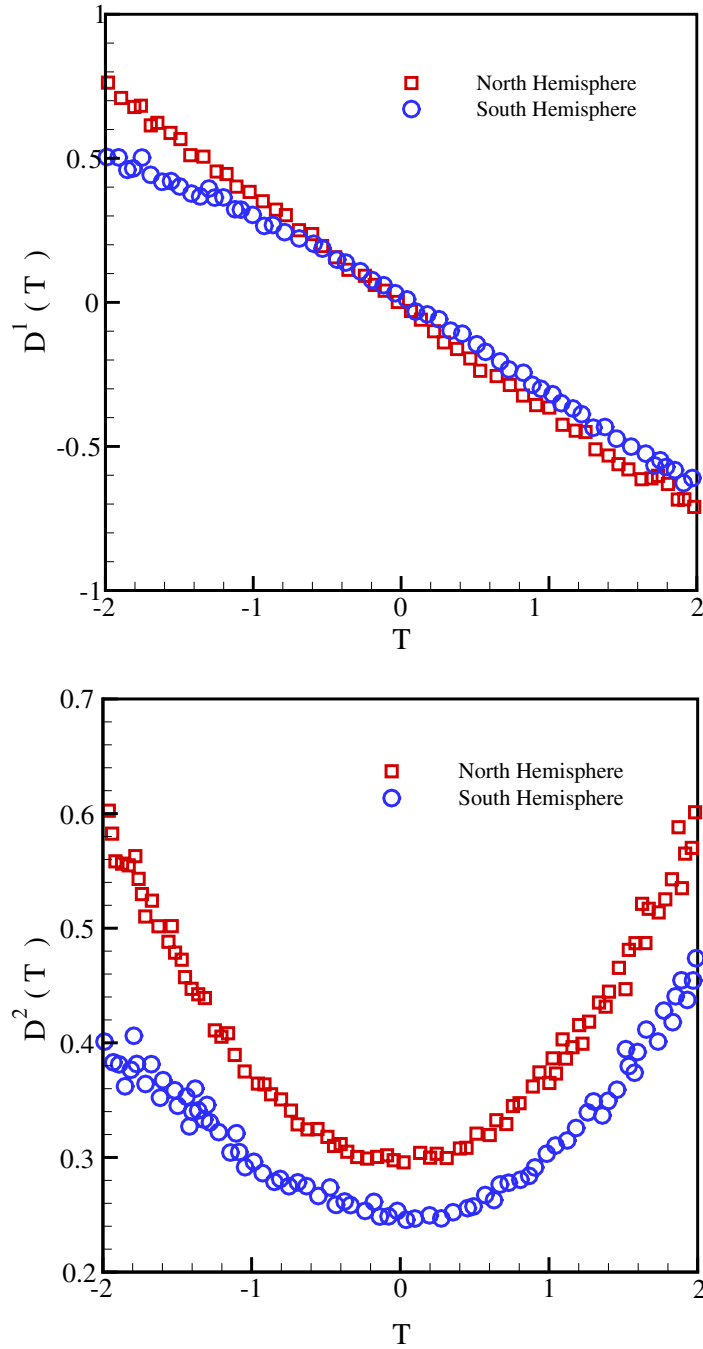


Figure 7. Drift and diffusion coefficients $D^{(1)}(T)$ and $D^{(2)}(T)$ for the northern and the southern hemisphere parts of the CMB data.

The second moment S_2 allows us to determine $\langle T(\hat{n}_1)T(\hat{n}_2) \rangle$ and, hence, the C_l . On the other hand, S_2 can be obtained through $P(\Delta T, \Theta)$, where $\Delta T = T(\hat{n}_1) - T(\hat{n}_2)$. The FP equation [16] for $\Delta T(\Theta)$ is given by

$$\frac{d}{d\Theta}P(\Delta T, \Theta) = \left[-\frac{\partial}{\partial \Delta T}D^{(1)}(\Delta T, \Theta) + \frac{\partial^2}{\partial \Delta T^2}D^{(2)}(\Delta T, \Theta) \right] P(\Delta T, \Theta). \quad (22)$$

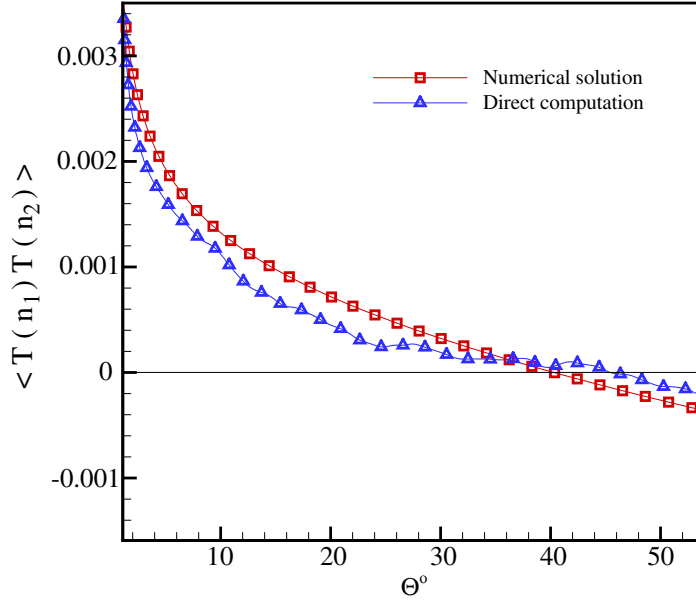


Figure 8. Comparison of the numerical solution of equation (24) and direct computation of $\langle T(\hat{n}_1)T(\hat{n}_2) \rangle$.

From the analysis of the CMB data we obtain the following equations for $D^{(1)}(\Delta T, \Theta)$ and $D^{(2)}(\Delta T, \Theta)$:

$$\begin{aligned} D^{(1)}(\Delta T, \Theta) &= \left(-0.190 - \frac{0.182}{\Theta} \right) \Delta T, \\ D^{(2)}(\Delta T, \Theta) &= \left[0.021 + 0.025 \exp \left(-\frac{\Theta}{8.896} \right) \right] (\Delta T)^2 + 0.279 + \frac{0.014}{\Theta^{0.429}}. \end{aligned} \quad (23)$$

Here, ΔT is measured in units of the standard deviation of T . Equation (22) allows us to obtain an equation for the second moment of the temperature increments, S_2 . Multiplying equation (22) by ΔT^2 and integrating over the increment of the temperature yields

$$\frac{d}{d\Theta} \langle T(\hat{n}_1)T(\hat{n}_2) \rangle = 2[\alpha(\Theta) + \omega(\Theta)] \langle T(\hat{n}_1)T(\hat{n}_2) \rangle - \sigma^2 [2\alpha(\Theta) + 2\omega(\Theta) - \beta(\Theta)], \quad (24)$$

where $\sigma^2 = \langle T^2 \rangle$, $D^{(1)}(\Delta T, \Theta) = \alpha(\Theta)\Delta T(\Theta)$, and $D^{(2)}(\Delta T, \Theta) = \beta(\Theta)\sigma^2 + \lambda(\Theta)\sigma\Delta T(\Theta) + \omega(\Theta)\Delta T(\Theta)^2$. The coefficients $\alpha(\Theta)$, $\beta(\Theta)$, $\lambda(\Theta)$, and $\omega(\Theta)$ are given by equation (23).

We obtain the correlation functions through numerical solution of equation (24) and compare them with the direct correlation shown in figure 8. The two approaches yield similar behaviour. At $\Theta \simeq 39^\circ$ the correlation function vanishes. The relation between the KM coefficients with C_l is then obtained by expanding the solution of equation (24) in terms of P_l .

6. Conclusion

We studied the stochastic nature of the temperature fluctuations in the CMB. The Markov angle, as the characteristic scale of the Markov properties of the CMB data, was obtained.

According to the theory of the stochastic process, the CMB data at scales larger than the Markov angle can be considered as a Markov process. This means that the data located at separations larger than the Markov scale can be described as a Markov chain. We also obtained the angular scale correlation for the CMB data and showed that it is independent of the Markov angular scale. This point can be explained as a simple example of Brownian motion. Its dynamics is described by the Langevin equation, $dv/dt = -\alpha v + \eta(t)$ (similar to equation (15)), where the force $\eta(t)$ is a zero-mean Gaussian white noise. It is known that this process is a Markov process with a Markov timescale of unity [16]. On the other hand, the correlation timescale is of the order of $1/\alpha$, which is the characteristic timescale in the Langevin equation [16]. This means that for a Markovian process the Markov timescale does not depend on the correlation timescale.

We showed that the probability density of the temperature increments satisfies a Fokker–Planck equation that encodes the Markov property of the fluctuations. We gave the expressions for the Kramers–Moyal coefficients of the stochastic process T and $\Delta T(\Theta)$, using the polynomial ansatz [58]–[63]. The Fokker–Planck equation enables us to derive a simple equation that governs the phenomenon in terms of azimuthal spherical coordinate. One of the important points that can be tested by this method is the notion of (non-) Gaussianity of the temperature field.

Using the Fokker–Planck equation, we obtained the relation between the fourth and the lower moments, and observed small deviations from the Gaussianity. The same calculation was carried out by dividing the data into the northern and southern hemispheres. The PDF of the temperature exhibits fat tails for the northern and the southern hemispheres. The third moment indicates that we have hot spots in the north, in contrast with the cold spots in the south hemisphere. To show a link between our method and the standard analysis of the CMB data through C_l calculation, we obtained the evolution equation for the correlation function through the Fokker–Planck equation that governs the temperature increments. We found good agreement between our method and that of direct correlation function calculation.

The most important result of this paper is a possible interpretation of the CMB data in terms of the Markov angular scale. In this work we computed the Markov angular scale for the temperature fluctuations in the CMB, in the range of $1.01^{+0.09}_{-0.07}$, where comparison with the event horizon shows that the two angles are of the same order of magnitude. A possible interpretation may be the physical connection of the Markov angular scale for the CMB data to the event horizon at the last scattering surface.

From the definition of the event horizon, two points located further apart than the Markov angular scale do not connect gravitationally. From the inflationary scenario for the early universe, all the points in the universe have been correlated during the inflationary epoch, and get an almost uniform Harrison–Zel’dovich spectrum. After the end of the inflation, the perturbation remaining from the inflation started to grow and the gravitational effect of each point could travel within the event horizon scales, so that outside the horizon we have the primordial spectrum from the inflation, while inside the horizon this spectrum has vanished due to the gravitational interaction between the points. The result is that, if we look at the density perturbation in the CMB as a stochastic field, the conditional probability of finding two points inside the event horizon scale will depend on all the particles in between, while for the points outside the event horizon, the memory of scale-invariant spectrum should be restored. A better interpretation of this

issue needs an N -body simulation of structure formation from the inflationary epoch to the last scattering surface, together with a simultaneous calculation of the Markov length.

Acknowledgments

We would like to acknowledge the WMAP team for providing us with their data. We thank R Ansari, H Arfaei, V Karimipour, R Mansouri, N Taghavinia, M A Vesaghi and M Sahimi for useful discussions. This work was supported by the Research Institute for Astronomy and Astrophysics of Maragha-Iran.

References

- [1] Afshordi N, Loh Y and Strauss M A, 2004 *Phys. Rev. D* **69** 083524
- [2] Bennett C L *et al*, 2003 *Astrophys. J. Suppl.* **148** 213
- [3] Spergel D N *et al*, 2003 *Astrophys. J. Suppl.* **148** 175
- [4] Tegmark M *et al*, 2004 *Phys. Rev. D* **69** 103501
- [5] Peiris H V *et al*, 2003 *Astrophys. J. Suppl.* **148** 213
- [6] Mukhanov V F and Chibisov G, 1981 *JETP Lett.* **33** 532
- [7] Hawking S W, 1982 *Phys. Lett. B* **115** 295
- [8] Guth A H and Pi S Y, 1985 *Phys. Rev. Lett.* **49** 1110
- [9] Bennett C L *et al*, 2003 *Astrophys. J.* **581** 1
- [10] Page L *et al*, 2003 *Astrophys. J. Suppl.* **148** 39
- [11] Peebles P J, 1980 *The Large Scale Structure of the Universe* (Princeton, NJ: Princeton University Press)
- [12] Donoghue E P and Donoghue J F, 2005 *Phys. Rev. D* **71** 043002
Hajian A, Souradeep T and Cornish N, 2004 *Astrophys. J.* **618** 63
Movahed S, Ghasemi F, Rahvar S and Rahimi Tabar M R, 2006 *Phys. Rev. D* submitted [[astro-ph/0602461](#)]
- [13] Friedrich R, Zeller J and Peinke J, 1998 *Europhys. Lett.* **41** 153
- [14] Jafari G R, Fazlei S M, Ghasemi F, Vaez Allaei S M, Rahimi Tabar M R, Iraj Zad A and Kavei G, 2003 *Phys. Rev. Lett.* **91** 226101
- [15] Ghasemi F, Peinke J, Sahimi M and Reza Rahimi Tabar M, 2005 *Eur. Phys. J. B* **47** 411
- [16] Risken H, 1984 *The Fokker–Planck Equation* (Berlin: Springer)
- [17] Colistete R Jr, Fabris J C, Gonçalves S V B and de Souza P E, 2004 *Int. J. Mod. Phys. D* **13** 669
- [18] Bardeen J M, Bond J R, Kaiser N and Szalay A S, 1986 *Astrophys. J.* **304** 15
- [19] Linde A and Mukhanov V F, *Nongaussian isocurvature perturbations from inflation*, 1997 *Phys. Rev. D* **56** 535
- [20] Peebles P J E, 1999 *Astrophys. J.* **510** 531
- [21] Peebles P J E, 1999 *Astrophys. J.* **510** 523
- [22] Antoniadis I, Mazur P O and Mottola E, *Comment on nongaussian isocurvature perturbations from inflation*, 1997 Preprint [astro-ph/9705200](#)
- [23] Fukushige T, Makino J, Nishimura O and Ebisuzaki T, 1995 *Publ. Astron. Soc. Japan* **47** 493
- [24] Bernardeau F, 1997 *Astron. Astrophys.* **324** 15
- [25] Banday A J, Górski K M, Bennett C L, Hinshaw G, Kogut A and Smoot G F, 1996 *Astrophys. J.* **468** L85
- [26] Tegmark M, 1997 *Astrophys. J.* **480** L87
- [27] Bond J R and Efstathiou G, 1987 *Mon. Not. R. Astron. Soc.* **226** 655
- [28] Coles P, 1988 *Mon. Not. R. Astron. Soc.* **234** 509
- [29] Smoot G F, Tenorio L, Kogut A and Wright E L, 1994 *Astrophys. J.* **437** 1
- [30] Kogut A and Banday A J, 1996 *Astrophys. J. Lett.* **464** L29
- [31] Winitzki S and Kosowsky A, 1997 *New Astron.* **3** 75
- [32] Bershadskii A and Sreenivasan K R, 2003 *Phys. Lett. A* **319** 21
- [33] Movahed S *et al*, 2006 Preprint [astro-ph/0602461](#)
- [34] Heavens A F, 1998 *Mon. Not. R. Astron. Soc.* **299** 805
- [35] Schmalzing J and Gorski K M, 1998 *Mon. Not. R. Astron. Soc.* **297** 355
- [36] Ferreira P G, Magueijo J and Gorski K M, 1998 *Astrophys. J. Lett.* **503** L1
- [37] Pando J, Valls-Gabaud D and Fang L Z, 1998 *Phys. Rev. Lett.* **81** 4568
- [38] Bromley B C and Tegmark M, 1999 *Astrophys. J. Lett.* **524** L79
- [39] Banday A J, Zaroubi S and Gorski K M, 2000 *Astrophys. J.* **533** 575
- [40] Contaldi C R, Ferreira P G, Magueijo J and Górski K M, 2000 *Astrophys. J.* **534** 25

- [41] Mukherjee P, Hobson M P and Lasenby A N, 2000 *Mon. Not. R. Astron. Soc.* **318** 1157
- [42] Magueijo J, 2000 *Astrophys. J. Lett.* **528** L57
- [43] Novikov D, Schmalzing J and Mukhanov V F, 2000 *Astron. Astrophys.* **364** 17
- [44] Sandvik H B and Magueijo J, 2001 *Mon. Not. R. Astron. Soc.* **325** 463
- [45] Magueijo J, 2000 *Astrophys. J. Lett.* **528** L57
- [46] Barreiro R B, Hobson M P, Lasenby A N, Banday A J, Górski K M and Hinshaw G, 2000 *Mon. Not. R. Astron. Soc.* **318** 475
- [47] Phillips N G and Kogut A, 2001 *Astrophys. J.* **548** 540
- [48] Komatsu E and Seljak U, 2002 *Mon. Not. R. Astron. Soc.* **336** 1256
- [49] Komatsu E and Spergel D N, 2001 *Phys. Rev. D* **63** 63002
- [50] Kunz M, Banday A J, Castro P G, Ferreira P G and Gorski K M, 2001 *Astrophys. J. Lett.* **563** L99
- [51] Aghanim N, Forni O and Bouchet F R, 2001 *Astron. Astrophys.* **365** 341
- [52] Cayón L, Martínez-González E, Argüeso F, Banday A J and Gorski K M, 2003 *Mon. Not. R. Astron. Soc.* **339** 1189
- [53] Park C, Ratra B and Tegmark M, 2001 *Astrophys. J.* **556** 582
- [54] Shandarin S F, Feldman H A, Xu Y and Tegmark M, 2002 *Astrophys. J. Suppl.* **141** 1
- [55] Wu J H *et al*, 2001 *Phys. Rev. Lett.* **87** 251303
- [56] Santos M G, Cooray A, Haiman Z, Knox L and Ma Ch, 2003 *Astrophys. J.* **598** 756
- [57] Polenta G *et al*, 2002 *Astrophys. J. Lett.* **572** L27
- [58] Friedrich R and Peinke J, 1997 *Phys. Rev. Lett.* **78** 863
- [59] Friedrich R, Peinke J and Renner C, 2000 *Phys. Rev. Lett.* **84** 5224
- [60] Friedrich R, Marzinzik K and Schmigel A, 1997 *A Perspective Look at Nonlinear Media (Springer Lecture notes in Physics vol 503)* ed J Parisi, S C Muller and W Zimmermann (Berlin: Springer) p 313
- [61] Davoudi J and Rahimi Tabar R M, 1999 *Phys. Rev. Lett.* **82** 1680
- [62] Ragwitz M and Kantz H, 2001 *Phys. Rev. Lett.* **87** 254501
- [63] Friedrich R, Renner C, Siefert M and Peinke J, 2002 *Phys. Rev. Lett.* **89** 149401